Since January 2020 Elsevier has created a COVID-19 resource centre with free information in English and Mandarin on the novel coronavirus COVID-19. The COVID-19 resource centre is hosted on Elsevier Connect, the company's public news and information website.

Bioorg. Med. Chem. Lett. 40 (2021) 127972

Contents lists available at ScienceDirect

Bioorganic & Medicinal Chemistry Letters

journal homepage: www.elsevier.com/locate/bmcl

SARS-CoV-2 main protease inhibition by compounds isolated from *Luffa cylindrica* using molecular docking

Thao Quyen Cao [a,c], Jeong Ah Kim [b], Mi Hee Woo [a], Byung Sun Min [a,*]

[a] College of Pharmacy, Drug Research and Development Center, Daegu Catholic University, Gyeongbuk 38430, Republic of Korea
[b] College of Pharmacy, Research Institute of Pharmaceutical Sciences, Kyungpook National University, Daegu 41566, Republic of Korea
[c] Institute of Pharmaceutical Research and Development, College of Pharmacy, Wonkwang University, Iksan 54538, Republic of Korea

ARTICLE INFO

Keywords:
Luffa cylindrical
Saponins
Valerolactone
SARS-CoV-2
Molecular docking

ABSTRACT

In this study, chemical investigation of methanol extract of the air-dried fruits of *Luffa cylindrica* led to the identification of a new *δ*-valerolactone (**1**), along with sixteen known compounds (**2**–**17**). Their chemical structures including the absolute configuration were elucidated by extensive spectroscopic analysis and electronic circular dichroism analysis, as well as by comparison with those reported in the literature. For the first time in literature, we have examined the binding potential of the isolated compounds to highly conserved protein, M^{pro} of SARS-CoV-2 using the molecular docking technique. We found that the isolated saponins (**14**–**17**) bind to the substrate-binding pocket of SARS-CoV-2 M^{pro} with docking energy scores of –7.13, –7.29, –7.47, and –7.54 kcal.mol^{-1}, respectively, along with binding abilities equivalent to an already claimed N3 protease inhibitor (–7.51 kcal.mol^{-1}).

Introduction

Luffa cylindrica, a subtropical vegetable, belonging to the Cucurbitaceae family, is also known as a vegetable sponge or sponge gourd. This plant is widely cultivated in Asia, India, Brazil, and the USA.[1] The fruits and seeds of *Luffa* contain various bioactive compounds, such as phenolics,[1] flavonoids,[1] luffins,[2,3] sapogenins,[4] and triterpenoids.[5] *Luffa* possesses wide pharmaceutical activities such as anticancer,[5] anti-inflammatory,[1] anti-HIV-1 (human immunodeficiency virus 1),[2] antioxidants,[6] antifungal,[7] and antibacterial[7] activities. For instance, oleanolic acid isolated from *L. cylindrica* demonstrated inhibition of NO production at 10 μM in an LPS/IFN-γ-induced cell model occurred.[8] It has been reported that the peptides, luffacylin and the peptide luffin *P*1 displays antifungal activity[9] and anti-HIV-1 activity,[2] respectively.

Towards the end of December 2019, a novel coronavirus (2019-nCoV/SARS-CoV-2) with human to human transmission, originated in Wuhan, China, and caused several human infections and disorders in the respiratory system.[10,11] This viral disease is a pandemic that has become a global challenge and the number of newly infected patients has been increasing day by day.[12] The coronavirus group comprises of numerous species and induces respiratory tract and gastrointestinal infections in vertebrates; nevertheless, some CoVs such as SARS, MERS, and SARS-CoV-2 have been reported to be especially dangerous to humans. Since the SARS-CoV-2 outbreak, different traditional herbs with promising results have been used alone or in combination with conventional drugs for the treatment of infected patients.[13] There exist numerous uncertainties surrounding the novel coronavirus behavior; thus, it is too early to conclude whether medicinal plants, spices, or isolated compounds and molecules could be used as preventive drugs or as appropriate therapeutic compounds against COVID-19.[14] However, the novel coronavirus SARS-CoV-2 and the previously reported viruses, MERS-CoV and SARS-CoV exhibit high similarity in genome sequences. Analysis of the genome sequences of these three viruses has revealed that SARS-CoV-2 has a higher identify with SARS-CoV (89.1% nucleotide similarity) than with MERS-CoV.[15] Hence, it is hypothesized that previous researches on phytomedicinal and herbal metabolites, which have been demonstrated to have anti-coronavirus properties, may be an appreciated guide to searching and discovering antiviral phytochemical extracts which may be effective against the SARS-CoV-2 virus.[14,16] We herein recommend a solution for the preclusion and treatment of the novel coronavirus by the isolated compounds from *L. cylindrica*.

A total of seventeen compounds (**1**–**17**) were isolated from the air-dried fruits of *L. cylindrica*, including one novel, 3,5-dihydroxy-*δ*-valerolactone (**1**). The details of the new compound are discussed below, and

* Corresponding author.
E-mail address: bsmin@cu.ac.kr (B.S. Min).

https://doi.org/10.1016/j.bmcl.2021.127972
Received 11 November 2020; Received in revised form 10 March 2021; Accepted 13 March 2021
Available online 19 March 2021

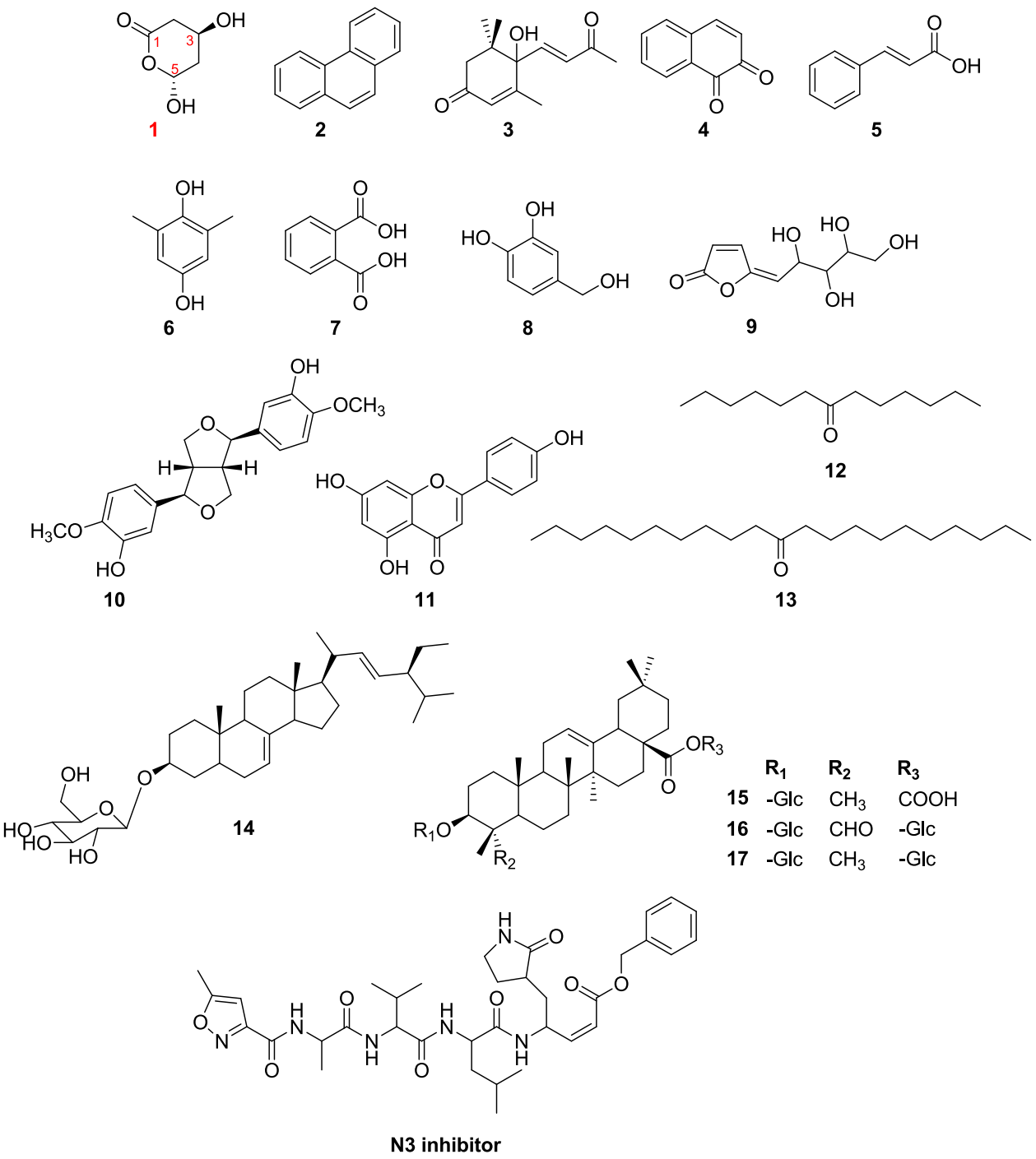

Fig. 1. Chemical structures of isolated compounds (1–17) from *L. cylindria* and N3 inhibitor.

the chemical structures of all the compounds are shown in Fig. 1.

Compound **1** was obtained as a colorless oil. The molecular formula of **1** as $C_5H_8O_4$, consistent with two degrees of unsaturation, was deduced from the HRESIMS spectrum showing the molecule ion mass peak at *m/z* 155.0320 $[M + Na]^+$ [calcd. for 155.0315]. The ^{13}C NMR spectrum of **1** showed the signal at δ_C 178.6, suggesting the presence of ester carbonyl moiety, which accounts for one degree of unsaturation. Besides that, two oxygenated methine carbons (δ_C 90.1 and 69.6) together with two methylene carbons (δ_C 62.4 and 39.1) were present in the ^{13}C NMR and DEPT spectra. Integration of the resonances in the ^1H NMR spectrum of **1** showed the presence of two oxymethine protons at δ_H 4.52 (1H, td, $J = 2.5$, 6.5 Hz, H-3) and 4.47 (1H, dd, $J = 3.5$, 5.5 Hz, H-5), and two methylene groups at δ_H 3.84 (1H, dd, $J = 3.5$, 12.5 Hz, H-

Table 1
^1H (500 MHz) and ^{13}C (125 MHz) NMR data in methanol-d_4 for compound 1.

No.	^1H (J in Hz)	^{13}C
1		178.6
2	2.47 dd (6.5, 18.0)	39.1
	3.01 dd (6.5, 18.0)	
3	4.52 dt (6.5, 2.5)	69.6
4	3.84 dd (3.5, 12.5)	62.4
	3.78 dd (3.5, 12.5)	
5	4.47 dd (3.5, 5.5)	90.1

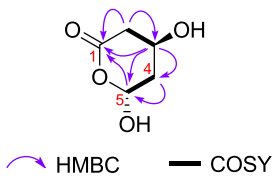

Fig. 2. Key HMBC and COSY correlations for 1.

4a), 3.78 (1H, dd, $J = 3.5, 12.5$ Hz, H-4b), 3.01 (1H, dd, $J = 6.5, 18.0$ Hz, H-2a), and 2.47 (1H, dd, $J = 2.5, 18.0$ Hz, H-2b) (Table 1). These data indicated **1** to be is a *δ*-valerolactone.[17] Analysis of HMQC and HMBC spectra, along with the comparison of the NMR data of **1** with those of 3-hydroxy-*δ*-valerolactone[17] suggested close structural similarity between the two compounds, except for the presence of a hydroxyl group in **1**. The location of the hydroxyl group at C-5 was supported by the key observation of HMBC correlations from H-5 to C-1, and H-3 and H-4 to C-5 (Fig. 2). Based on these evidences, the planar structure of **1** was elucidated as 3,5-dihydroxy-*δ*-valerolactone.

Protons H-4 and H-5 displayed a small coupling constant ($^3J_{H\text{-}4,H\text{-}5}$ = 3.5 Hz), which is consistent with a *gauche* conformation[18] (Fig. S1). The NOESY spectrum of **1** displayed no spatial correlation between oxymethine protons H-3 and H-5, indicating two cases for configuration of (3*S*,5*R*)-**1** and (3*R*,5*S*)-**1** (Fig. S1). Furthermore, the electronic circular dichroism (ECD) spectra calculations for both **1** and its enantiomer were carried out using the time-dependent density functional theory (TDDFT) method.[19] The experimental ECD curves of **1** correlated well with that calculated for (3*S*,5*R*)-**1** in the range of 200 to 242 nm (Fig. 3). Consequently, the structure of **1** was conclusively determined to be (3*S*,5*R*)-dihydroxy-*δ*-valerolactone.

The other compounds were identified as phenanthrene (**2**),[20] (*S*)-dehydrovomifoliol (**3**),[21] 1,2-naphthoquinone (**4**),[22] cinnamic acid (**5**),[23] 2,6-dimethyl-1,4-benzenediol (**6**),[24] phthalic acid (**7**),[25] 4-(hydroxymethyl)benzene-1,2-diol (**8**),[26] litchiol B (**9**),[27] pinoresinol (**10**),[28] apigenin (**11**),[29] tridecan-7-one (**12**),[30] henicosan-11-one (**13**),[30] 3-*O*-*β*-D-glucopyranosyl-spinasterol (**14**),[31] 3-*O*-*β*-D-glucopyranosyl-oleanolic acid (**15**),[32] lucyoside F (**16**),[33] and lucyoside H (**17**),[33] by comparison of their spectral data with values reported in the literature. To the best of our knowledge, compounds **3** and **9** were reported the first time from *Luffa* species. Compound **14** was isolated from *L. cylindrica* for the first time.

Along with various structural proteins, all the CoV genomes encode for a critical viral component called Main Protease (M^{pro}).[34] The latter is a 306 amino acids long enzyme that mainly helps in the replication of the virus through proteolytic processing of its RNA replicase machinery. M^{pro} from different human and animal CoVs have been shown to possess high similarity in terms of the primary amino acid sequence as well as the functional tertiary conformation of the enzyme.[35] The recently discovered SARS-CoV-2 also shares the homology in its M^{pro} enzyme.[36] Thus, we have employed M^{pro} as a target. Also, N3 holds the potential to specifically inhibit M^{pro} from multiple coronaviruses and has previously displayed potent antiviral activity against infectious bronchitis virus in an animal model.[37] The structure of the N3 inhibitor co-crystalized with the M^{pro} of SARS-CoV-2, which was recently released in Protein Data Bank (PDB) (6LU7),[43] gave us insights into the molecular mechanism of N3 inhibitor action against the new coronavirus.[34]

In this study, we demonstrate docking molecules of the isolated compounds (**1**–**17**) and N3 inhibitor into the PDB6LU7 protein (Fig. 4) using PyRx 0.9.4 virtual screening software,[44] to contribute to the orientation and encourage the use of natural metabolites for SARS-CoV-

Fig. 4. PDB6LU7 Protein in SARS-CoV-2 Main Protease.

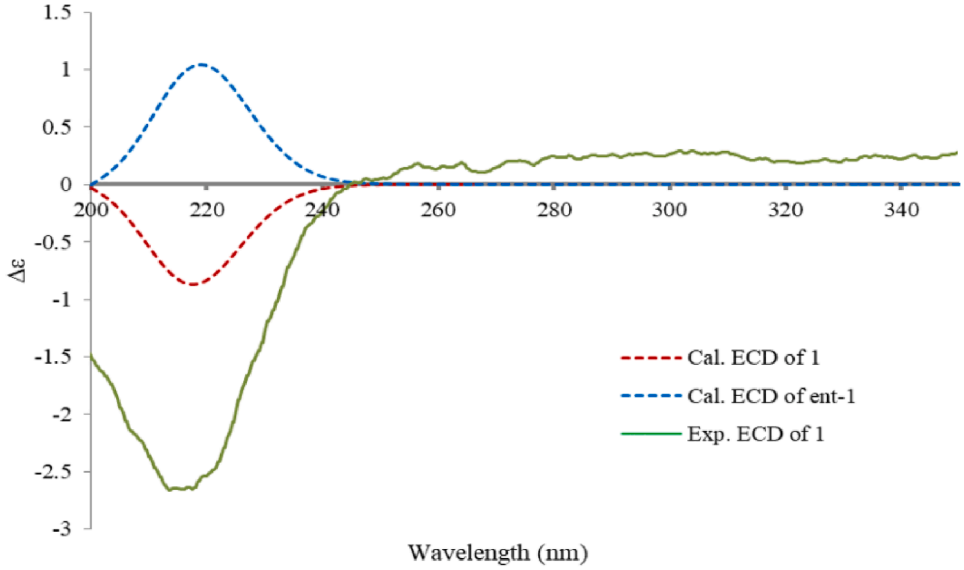

Fig. 3. Experimental and calculated ECD spectra of 1.

Table 2
Docking simulation results with docking score energy (DS) and root-mean-square deviation (RMSD) between isolated compounds (**1**, **3**–**11**, and **14**–**17**) and the PDB6LU7 protein.

Compounds	DS (kcal.mol^{-1})	RMSD (Å)	Interaction with amino acid
1	–4.68	32.97	His 163 (2.1 Å), Gly 143 (2.7 Å), Cys 145 (2.5 Å), Ser 144 (2.1 Å), Asn 142 (2.1 Å)
3	–5.08	21.49	Asn 151 (2.5 Å)
4	–5.37	15.77	Gln 110 (2.3 Å)
5	–4.83	15.03	Asn 151 (2.2 Å), Thr 111 (2.3 Å)
6	–4.89	15.05	Thr 111 (2.2 Å), Gln 110 (2.6 Å)
7	–5.52	0.64	Asn 151 (2.7 Å), Gln 110 (2.2 Å), Thr 111 (2.2 Å), Asr 195 (2.6 Å)
8	–4.78	15.84	Gly 275 (1.8 Å), Arg 279 (2.0 Å), Phe 219 (2.4 Å), Leu 220 (2.4 Å)
9	–5.09	12.38	His 41 (2.4 Å), Glu 166 (2.1 Å), His 163 (2.2 Å)
10	–6.76	22.19	Asn 151 (2.5 Å)
11	–6.77	16.34	Gln 192 (2.6 Å), Glu 166 (2.3 Å), His 163 (2.5 Å), Ser 144 (2.6 Å)
14	–7.13	13.48	Thr 199 (2.6 Å), Asr 289 (2.2 Å), Arg 131 (2.2 Å), Asr 197 (2.1 Å), Lys 137 (2.3 Å)
15	–7.29	19.90	Thr 199 (1.9 Å), Asn 238 (2.6 Å), Lys 137 (2.5 Å)
16	–7.47	15.71	Leu 272 (1.8 Å), Thr 199 (2.5 Å), Asr 289 (2.7 Å)
17	–7.54	7.77	Lys 137 (2.3 Å), Leu 287 (1.8 Å), Ala 285 (2.3 Å), Met 276 (1.9 Å), Asn 277 (2.0 Å)
N3	–7.51	16.51	Arg 105 (2.7 Å), Gln 110 (2.2 Å)

2 inhibition. The docking was successful in fifteen compounds **1**, **3**–**11**, **14**–**17**, and N3 inhibitor. The results of docking score energy (DS) and root mean square deviation (RMSD) between the fifteen compounds and protein with various interactions, including hydrogen bonds interactions and the interaction distance between amino acids and the active sites of compounds are shown in Table 2.

We re-docked the N3 inhibitor in the same configuration to get a docking score for the natural binding. The docking score was found to be –7.51 kcal.mol^{-1} and was used to compare the binding of the isolated compounds with the M^{pro} of SAR-CoV-2. The two main residues that formed polar interaction with the inhibitor were Arg105 and Gln110 (Fig. 5A). A grid was generated around the conserved residues of the substrate-binding pocket with the main emphasis on the residues making polar contacts with the N3 inhibitor. Subsequently, the isolated compounds were then docked using the same grid. From the docking results, it was observed that lucyoside H (**17**), an oleanane saponin demonstrated –7.54 kcal.mol^{-1} binding energy with eight hydrogen bonds and interaction with five residues, Ala285, Lys137, Asn277, Met276, and Leu287 (Fig. 5E), thereby providing dramatic and approximate effect on the anti-SAR-CoV-2 activity along with N3 inhibitor. The other oleanane saponin, lucyoside F (**16**) displayed a slightly lower effect on the protein than compound **17** and N3 inhibitor with a binding energy value of –7.47 kcal.mol^{-1} with four hydrogen bonds and interacted with three residues, Asr289, Thr199, and Leu272 (Fig. 5D). Saponins **14** and **15** showed a significant effect on the protein of SARS-CoV-2 with the binding energy of –7.13 and –7.29 kcal.mol^{-1}, respectively. As illustrated in Fig. 5B, the corresponding ligand interactions of **14** with the virus protein were five hydrogen-bonding interactions with the Thr199, Lys137, Asr289, Arg131, and Asr197 residues with the bond distances of 2.6, 2.3, 2.2, 2.2, and 2.1 Å, respectively. Compound **15** displayed the effect by three hydrogen binding bonds and three interacting residues of Asn238, Lys137, and Thr199 with the bond distances of 2.6, 2.5, and 1.9 Å, respectively (Fig. 5C). These results showed that compounds **14** and **15** shared the same residues (Thr199 and Lys137) *via* the interaction with the SARS-CoV-2 protein. Besides that, compounds **10** and **11** revealed a noticeable effect on the PDB6LU7 protein with the binding energy values of –6.76 and –6.77 kcal.mol^{-1} (Table 2). Compound **10** exhibited the activity by only one hydrogen binding bond and an interacting residue Asn151 with the bonding distance of 2.5 Å. Meanwhile, the activity of compound **11** was deciphered by binding to four hydrogen bonds as well as interacting with four residues Gln192, Ser144, His163, and Glu166 with the bond distance values of 2.6, 2.6, 2.5, and 2.3 Å, respectively (Table 2). The other compounds **1** and **3**–**9** showed a moderate effect on the protein of SARS-CoV-2 with the binding energy values of –4.68, –5.08, –5.37, –4.83, –4.89, –5.52, –4.78, and –5.09 kcal.mol^{-1}, respectively (Table 2).

The above-mentioned data showed that saponins had the most potent effect on the SARS-CoV-2 inhibition. Interestingly, all of the corresponding ligand interactions of saponins **14**–**17** with PDB6LU7 protein were the hydrogen-bonding interactions between the enzyme residues and the hydroxyl groups in the sugar rings of these compounds (Fig. 5). Consequently, the key role of the glycosyl group in the SARS-CoV-2 inhibition was indicated. Among the isolated saponins, compound **14** is a sterol saponin, that demonstrated a lower effect than oleanane saponins **15**–**17**, thereby suggesting that the nature of aglycone in saponins might be a crucial factor in mediating the inhibition of SARS-CoV-2. Saponins are widely distributed in the plant kingdom and have been reported to possess a large number of biological activities, including anti-inflammation,[38] anti-cancer,[39] antioxidant,[40] anti-HIV,[41] as well as anti-viral.[42] Additionally, compound **17** that differs from compound **16** by a methyl group at the position of C-23, exhibited higher activity against COVID-19 protein than compound **16**. This result indicated that the presence of the methyl group at C-23 can increase SARS-CoV-2 inhibitory activities. Furthermore, the glycosyl group at C-28 in compound **17** that was changed by the carboxyl group in compound **15** demonstrated a lower effect on the PDB6LU7 protein. Thus, it is proposed that the number of glycosyl groups in the saponins structure might have an impact on the SARS-CoV-2 inhibitory effect of saponins. On the other hand, compounds **10** and **11** that are a lignan and a flavonoid, respectively, displayed quite similar inhibitory activity, thereby demonstrating a similar ability to inhibit the SARS-CoV-2 protein of lignans and flavonoids. Consequently, the above-mentioned evidences might support for the crucial role of saponins in the anti-coronavirus drug studies.

In conclude, we isolated a new δ-valerolactone (**1**), together with sixteen known compounds (**2**–**17**) from the extract of *L. cylindrica* fruits. The isolated compounds were compared for the SARS-CoV-2 inhibitory ability through PDB6LU7 protein to N3 inhibitor by using the molecular docking technique. All the isolated saponins (**14**–**17**) displayed the remarkable binding abilities into the pocket of SARS-CoV-2 M^{pro} with docking energy scores of –7.13, –7.29, –7.47, and –7.54 kcal.mol^{-1}, respectively. Consequently, these findings provide the direction of research and application of the natural products in general and components isolated from *L. cylindrica* isolated components in particular, in the prevention and treatment of SARS-CoV-2.

Declaration of Competing Interest

The authors declare that they have no known competing financial interests or personal relationships that could have appeared to influence the work reported in this paper.

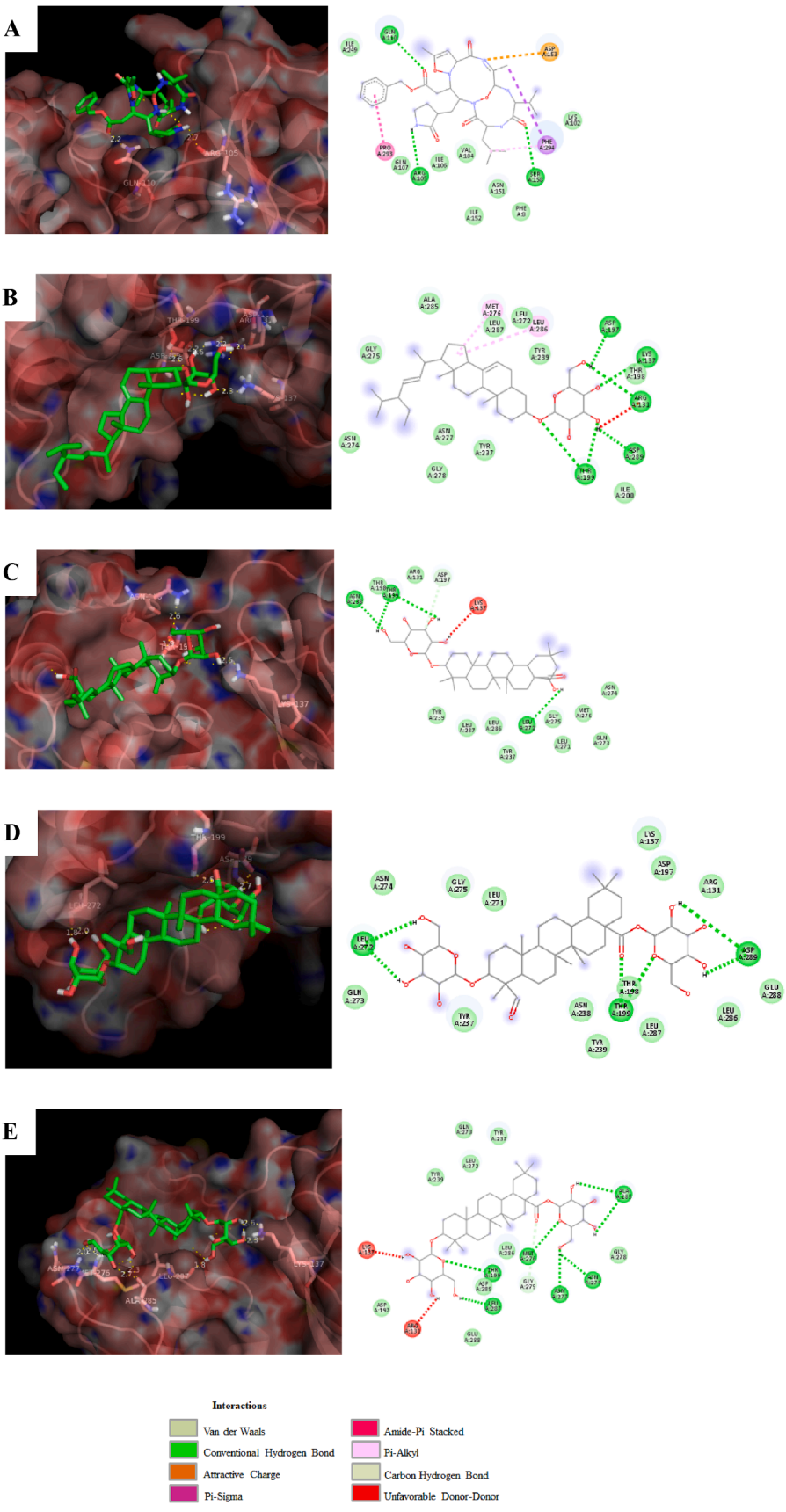

Fig. 5. Docking simulation of the interactions between N3 inhibitor, and compounds 14–17 and the PDB6LU7 protein of SARS-CoV-2 (A–E).

Acknowledgements

This research was supported by the National Research Foundation of Korea (NRF) funded by the Ministry of Science and ICT (2020R1F1A1072001), Korea. We are grateful to the Korea Basic Science Institute (KBSI) for mass spectrometric measurements.

Appendix A. Supplementary data

Supplementary data to this article can be found online at https://doi.org/10.1016/j.bmcl.2021.127972.

References

1 Kao TH, Huang CW, Chen BH. *Food Chem.* 2012;135(2):386–395.
2 Ng YM, Yang Y, Sze KH, et al. *J Struct Biol.* 2011;174(1):164–172.
3 Parkash A, Ng TB, Tso WW. *Peptides.* 2002;23(6):1019–1024.
4 Ha H, Lim HS, Lee MY, et al. *Pharm Biol.* 2015;53(4):555–562.
5 Azeez MA, Bello OS, Adedeji AO. *J Med Plants Stud.* 2013;1(5):102–111.
6 Pimple BP, Kadam PV, Patril MJ. *Asian Pac J Trop Med.* 2012;5(8):610–615.
7 Al-Snafi AE. *IOSR J Pharm.* 2019;9(9):68–79.
8 Honda T, Finlay HJ, Gribble GW, Suh N, Sporn MB. *Bioorg Med Chem Lett.* 1997;7(13):1623–1628.
9 Umehara M, Yamamoto T, Ito R, et al. *J Funct Foods.* 2018;40:477–483.
10 Chikhale RV, Sinha SK, Patil RB, et al. *J Biomol Struct Dyn.*. 2020:1–15.
11 Zhang DH, Wu KL, Zhang X, Deng SQ, Peng B. *J Integr Med.* 2020;18(2):152–158.
12 Chen J. *Microbes Infect.* 2020;22(2):69–71.
13 Benarba B, Pandiella A. *Front Pharmacol.* 2020;11:1–16.
14 Boukhatem MN, Setzer WN. *Plants.* 2020;9(6):1–23.
15 Wu F, Zhao S, Yu B, et al. *Nature.* 2020;579:265–269.
16 Chikhale RV, Gurav SS, Patil RB, et al. *J Biomol Struct Dyn.*. 2020:1–12.
17 Miyashita M, Suzuki T, Hoshino M, Yoshikoshi A. *Tetrahedron.* 1997;53(37):12469–12486.
18 George EC, Pham HT, Nguyen VH, et al. *J Nat Prod.* 2010;73:784–787.
19 Vu VT, Nguyen MT, Wang WL, et al. *Org Biomol Chem.* 2020;18:6607–6611.
20 Lutnaes BF, Luthe G, Brinkman UAT, Johansen JE, Krane J. *Magn Reson Chem.* 2005;43(7):588–594.
21 Yang Y, Bakri M, Gu D, Aisa HA. *J Liq Chromatogr Relat.* 2013;36(5):573–582.
22 Smithgall TE, Harvey RG, Penning TM. *J Biol Chem.* 1988;263(4):1814–1820.
23 Li K, Bi KS. *Chem Res Chinese U.* 2006;22(1):56–60.
24 Porkhun VI, Aristova YV, Gonik IL. *Russ Chem.* 2018;67:1364–1368.
25 Remko M. *Chem Zvesti.* 1975;29(3):387–391.
26 Pyne SG, Truscott RJW, Maxwell K, et al. *Tetrahedron.* 1990;46(2):661–670.
27 Wang L, Lou G, Ma Z, Liu X. *Food Chem.* 2011;126(3):1081–1087.
28 Cao TQ, Tran MH, Kim JA, et al. *Bioorg Med Chem Lett.* 2015;25(22):5087–5091.
29 Alwahsh MAA, Khairuddean M, Chong WK. *Rec Nat Prod.* 2015;9(1):159–163.
30 Tanaka K, Matsui S, Kaji A. *Bull Chem Soc Jpn.* 1980;53(12):3619–3622.
31 Zhang LJ, Yang XD, Xu LZ, Zou ZM, Yang SL. *J Asian Nat Prod Res.* 2005;7(4):649–653.
32 An RB, Na MK, Min BS, Lee HK, Bae KH. *Nat Prod Sci.* 2008;14(4):249–253.
33 Takemoto T, Arihara S, Yoshikawa K, et al. *Yakugaku Zasshi.* 1984;104(3):246–255.
34 Jin Z, Du X, Xu Y, et al. *Nature.* 2020;582(7811):289–293.
35 Woo PC, Huang Y, Lau SK, Yuen KY. *Viruses.* 2010;2(8):1804–1820.
36 t(.//sb:host[1]//child::*//sb:date)">Kumar V, Dhanjal JK, Kaul SC, Wadhwa R, Sundar D. *J Biomol Struct Dyn.*. 2020:1–13.
37 Xue X, Yu H, Yang H, et al. *J Virol.* 2008;82(5):2515–2527.
38 Lee TH, Jung M, Bang MH, Chung DK, Kim J. *Int Immunopharmacol.* 2012;13(3):264–270.
39 Liu CY, Hwang TL, Lin MR, et al. *Mar Drugs.* 2010;8(7):2014–2020.
40 Kim YA, Kong CS, Lee JI, et al. *Bioorg Med Chem Lett.* 2012;22(13):4318–4322.
41 Yogeeswari P, Sriram D. *Curr Med Chem.* 2005;12(6):657–666.
42 Zhou M, Xu M, Ma XX, et al. *Planta Med.* 2012;78(15):1702–1705.
43 Yu R, Chen L, Lan R, Shen R, Li P. *Int J Antimicrob Agents.* 2020;56(2):1–6.
44 Dallakyan S, Olson AJ. *Methods Mol Biol.* 2015;1263:243–250.